eJNDT e-Journal of Nondestructive Testing - ISSN 1435-4934 - www.ndt.net

EWSHM 2024
11th European Workshop on Structural Health Monitoring

Increased Accuracy of Service Life Prediction for Fiber Metal Laminates by Consideration of the Manufacturing-Induced Residual Stress State

Johannes WIEDEMANN[1], Selim MRZLJAK [2], Christian HÜHNE[1], Frank WALTHER [2]

[1] Technische Universität Braunschweig, Institute of Mechanics and Adaptronics, Braunschweig, Germany (johannes.wiedemann@tu-braunschweig.de)
[2] TU Dortmund University, Chair of Materials Test Engineering (WPT), Dortmund, Germany

Abstract. Fiber metal laminates (FML) combine the high specific properties of fiber-reinforced polymers with the ductility and damage tolerance of metals. However, during the manufacturing process of FMLs, in-plane residual stresses arise in the single layers of the laminate. The stresses mainly originate from the different coefficients of thermal expansion of the two materials and lead to an inhomogeneous stress state in the thickness direction of the laminate.

This work investigates the influence of such thermal residual stress (TRS) on the fatigue life in an FML by experimentally varying the TRS in identical layups using modified cure cycles. The experimental investigations show that the amount of TRS directly influences the fatigue performance of such laminates. Reducing the TRS, particularly the tensile residual stresses in the metal layers, slows the fatigue crack growth during cyclic loading. This leads to a significantly delayed crack initiation and slower crack propagation.

Knowledge of material behavior is essential for utilizing the full potential of structural health monitoring (SHM) in component lifetime predictions. Predictive models require a set of input parameters to perform this task. Since the TRS in an FML significantly contributes to the component's fatigue life, its consideration in predictive approaches is inevitable. This finding is discussed based on a phenomenological damage accumulation model initially developed for composite materials.

Keywords: fiber metal laminates, structural health monitoring, thermal residual stress, fatigue damage evolution

Introduction

Fiber-metal laminates (FML) are a class of composite materials that offer the benefits of both fiber-reinforced polymers (FRP) and metals. The development of FML can be traced back to

https://doi.org/10.58286/29832

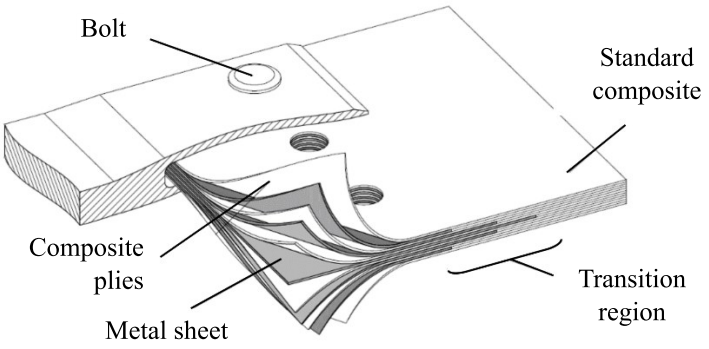

Fig. 1: Application example for CFRP-steel laminates [1]

two basic ideas that led to various combinations of FRP and metal. Firstly, adding layers of glass fiber-reinforced plastic significantly enhanced the fatigue resistance of pure aluminum structures, leading to the industrial application of this material named GLARE in the Airbus A380. Secondly, adding metallic layers to areas susceptible to load transfer and impact could make the brittle and less damage-tolerant monolithic fiber composite much more robust, mainly when using carbon fiber-reinforced plastics. An application of such an FML is shown in Fig. 1, where the FRP is locally reinforced near a bolted joint by substituting FRP plies with metal layers, leading to a significantly increased bearing strength of the composite and a more damage-tolerant structure.

However, the process temperatures during manufacturing of high-performance composite materials, and the significant differences in the coefficient of thermal expansion (CTE) and stiffness of metal and FRP lead to the development of a thermally induced interlaminar residual stress state, which reduces the theoretical material performance. Fig. 2 shows that the thermal residual stress (TRS) typically leads to tensile stress in the metal sheets and compressive stress in the FRP layers.

Investigations in GLARE show that post-stretching of laminates after manufacturing can change the TRS state into a more favorable stress state, significantly influencing the evolution of fatigue damage [2]. However, post-stretching operations are not practical for most industrial components, including those depicted in Fig. 1. As a result, there has been a growing interest in using modified cure cycles to reduce TRS in an FML, which showed to significantly increase the quasi-static strength of such CFRP-steel laminates [3].

Fig. 1 implies that applications of this nature require a high level of structural integrity. One way to ensure this integrity during operation is by implementing a structural health monitoring (SHM) system. For optimal results, an SHM system should identify and locate damage while also predicting the remaining service life of the component and when repairs are needed as illustrated in Fig. 3. For composite structures with large in-plane

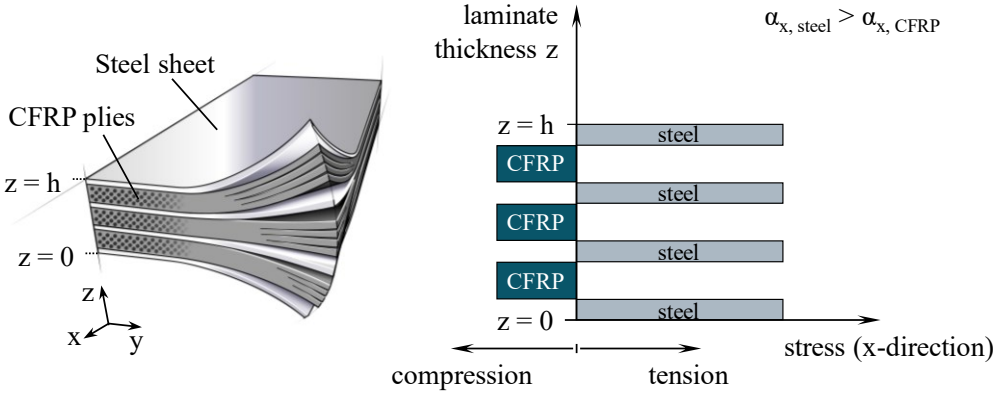

Fig. 2: Thermal residual stress state in a CFRP-steel laminate after manufacturing

Fig. 3: Tasks for a structural health monitoring system to perform

dimensions and limited thickness typical for aerospace, using guided ultrasonic waves (GUW) has proven to be a potent tool to diagnose the state of health. [4]

Unlike monolithic metals and FRP, FML has a highly anisotropic and inhomogeneous structure due to the significant differences in stiffness between metal and FRP. This leads to large inhomogeneities, especially in the thickness direction with high impedance differences and highly complex in-plane displacements of propagating GUW [5]. However, the literature indicates that damage detection in FML using SHM systems based on GUW is possible [6], and fundamental assumptions for Lamb wave propagation in layered media are valid [7,8].

Regarding damage localization, previous work has shown that TRS does not significantly impact the dispersion behavior of GUW in CFRP-steel within the frequency range studied and both the fundamental symmetric (S_0) and antisymmetric (A_0) modes [9,10]. As a result, it can be assumed that TRS in FML does not adversely affect damage localization methods that depend on the wave propagation velocity.

The evolution of fatigue damage plays a decisive role in service life predictions after damage detection and localization. However, little literature exists on the influence of differing TRS due to modified cure cycles on fatigue in FML. Therefore, this work aims to investigate the influence of TRS on fatigue damage evolution and the consequences for service life predictions using SHM for FML.

1. Materials and Methods

TRS in FMLs mainly develops during the manufacturing process when the laminate is cooled to room temperature after bonding at elevated temperature due to the difference in CTE and stiffness between metal and FRP (cf. Tab. 1). The CFRP material used in this work must be cured at 180°C as indicated by the manufacturer's recommended cure cycle (MRCC). This leads to a stress-free temperature of the final laminate close to the maximum curing temperature. Introducing an intermediate cooling step within a modified cure cycle (MOD) can significantly reduce the stress-free temperature and, thus, the TRS [11]. For the two cure cycles used in this work, the stress-free temperatures for the MRCC and MOD cycle are 178°C and 136°C, respectively. Details on the cure cycles and determining the stress-free temperatures can be found in previous publications [12,13].

Tab. 1: Material parameters for the steel and CFRP material used in this work

Parameter	Steel 1.4310 (X10CrNi18-8)	Hexcel Hexply 8552-AS4	Unit
E_1	191	122	GPa
E_2	191	9.9	GPa
ν_{12}	0.3	0.27	-
G_{12}	73.5	5.2	GPa
α_1	19.0×10^{-6}	0.4×10^{-6}	K^{-1}
α_2	19.0×10^{-6}	31.2×10^{-6}	K^{-1}

With these two manufacturing processes and the materials in Tab. 1, two different FML layups, labeled ID2 and ID6b, are manufactured. Details on the layups can be found in Tab. 2. The two layups differ in the total laminate thickness, the thickness of the steel sheets,

and, consequently, the metal volume fraction (MVF). The thickness of a single CFRP ply is 0.13 mm for both laminates.

Tab. 2: FML layups investigated in this work

ID	Layup	FML thickness	Steel sheet thickness	Metal volume fraction
2	$[St/0°_4/St/0°_2]_s$	2.04 mm	0.12 mm	23.5 %
6b	$[(St/0°_4)_3/\overline{St}]_s$	4.87 mm	0.25 mm	35.9 %

For fatigue testing, the manufactured laminates are cut into rectangular specimens with a length of 180 mm and a width of 20 mm using water jet cutting. Additionally, a 5 mm hole is drilled into the center of each specimen to initiate an early crack in the reduced specimen's cross-section.

The notched specimens are tested in a servo-hydraulic testing system with a sinusoidal load and a fixed stress ratio of R = 0.1 (tensile-tensile loading). For the constant amplitude tests, two different maximum stress levels σ_{max} (400 MPa and 600 MPa) are used, and the testing frequency is set to 10 Hz for all tests to minimize specimen self-heating while simultaneously keeping test time within reason.

During the fatigue tests, the force (F) and displacement (s) of the testing machine are continuously recorded to calculate the dynamic stiffness C_{dyn} of the specimen:

$$C_{dyn} = \frac{F_{max} - F_{min}}{s_{max} - s_{min}} \tag{1}$$

Additionally, the specimen's surface temperature is recorded with a thermographic camera (Infratec ImageIR 8800), and the specimen's surface is monitored with a digital image correlation (DIC) system (Limess Q400 3D-DIC), both of which are triggered at maximum stress during testing.

2. Combined Thermal and Mechanical Stresses in the Laminates

Using classical laminate theory (CLT) (e.g. [14]), the material parameters (Tab. 1), the cure cycle-specific stress-free temperatures, and the maximum stress levels during testing, the stresses in the single layers of the FML are calculated. Fig. 4 shows the stresses per ply for layup ID6b for an external laminate stress of 400 MPa, dependent on the cure cycle. The total ply stresses are a superposition of the TRS after manufacturing and the stresses due to external loads on the laminate. It can be seen that the TRS in the metal layers already accounts for more than a third of the total metal ply stresses when applying an external load of 400 MPa on the ID6b MRCC specimen. Using modified cure cycles (MOD), the TRS and, hence, the total stress in the metal layers of a specimen can be significantly reduced.

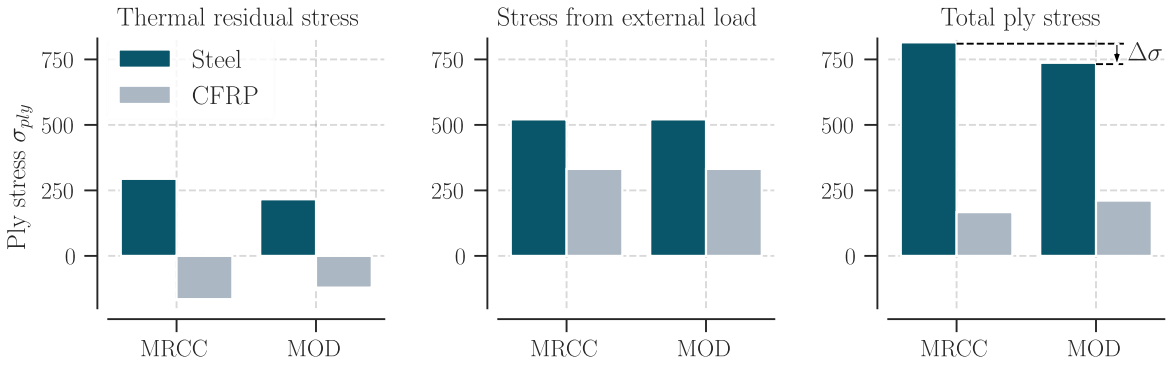

Fig. 4: Total ply stresses in the metal and FRP plies of an FML are a superposition of thermal residual stresses and stress from external loads (here: layup ID6b and σ_{max} = 400 MPa)

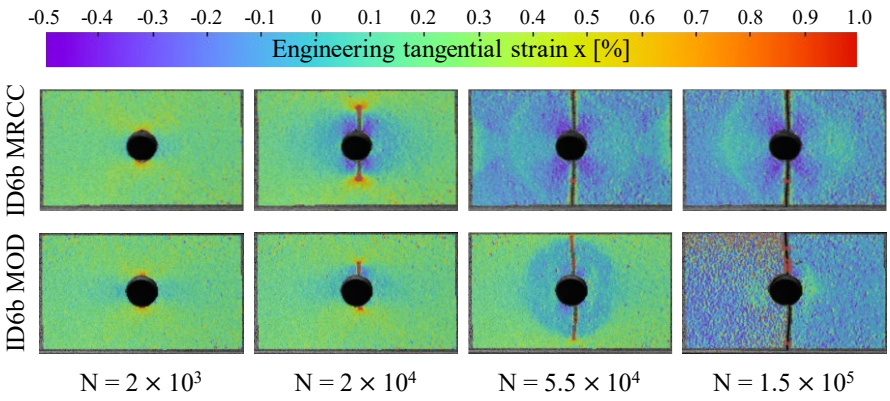

Fig. 5: DIC images for selected numbers of cycles show the difference in damage evolution in the top metal ply of specimens with layup ID6b and two different thermal residual stress states

3. Damage Evolution during Fatigue Testing

The fatigue test results show that the crack initiation and propagation are significantly delayed for the laminates with reduced TRS (MOD). This can be seen in the evaluation of the DIC images of the top steel sheet in Fig. 5. After 2×10^4 cycles, the crack length for specimen ID6b MOD (bottom) is smaller, and complete ply failure has not yet occurred after 5.5×10^4 cycles as compared to the MRCC specimen (top).

Fig. 6 further quantifies this delayed and prolonged crack growth for specimens with reduced residual stresses for all investigated layups. The specimens manufactured with the MOD cure cycle show a significantly increased number of cycles between crack initiation and failure of the outer metal sheets for both fatigue load scenarios.

From composite materials, it is known that damage accumulates during fatigue loading while the damage growth rate is not constant all over the component's fatigue life. The damage accumulation is accompanied by a decrease in specimen stiffness. Evaluating the dynamic stiffness according to Equation (1) over the number of cycles N in the fatigue tests, a reduction in stiffness is found for all specimens, as shown exemplarily for layup ID6b in Fig. 7. The change in specimen temperature during the constant amplitude tests correlates inversely with the normalized dynamic stiffness of the specimen. Both variables can characterize the damage evolution during fatigue testing. The specimens with different TRS show a significant difference in damage evolution. While the initial decrease in normalized dynamic stiffness is comparable for the MRCC and MOD specimens, damage accumulates much faster in the specimen with higher TRS (MRCC) after the outer metal sheets fail.

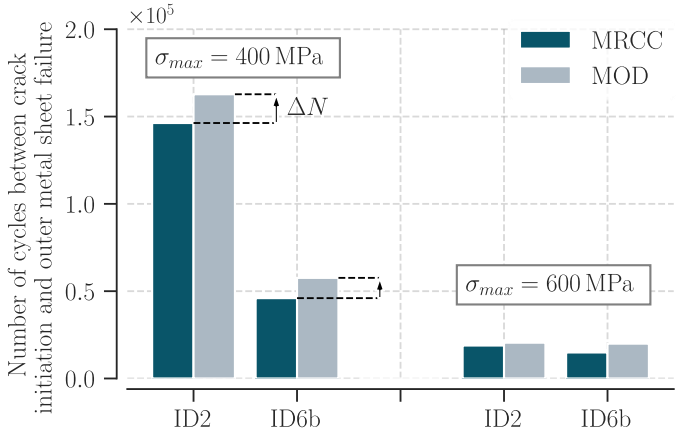

Fig. 6: Reduced thermal residual stress leads to an increase in cycles between crack initiation and outer metal sheet failure for all investigated configurations

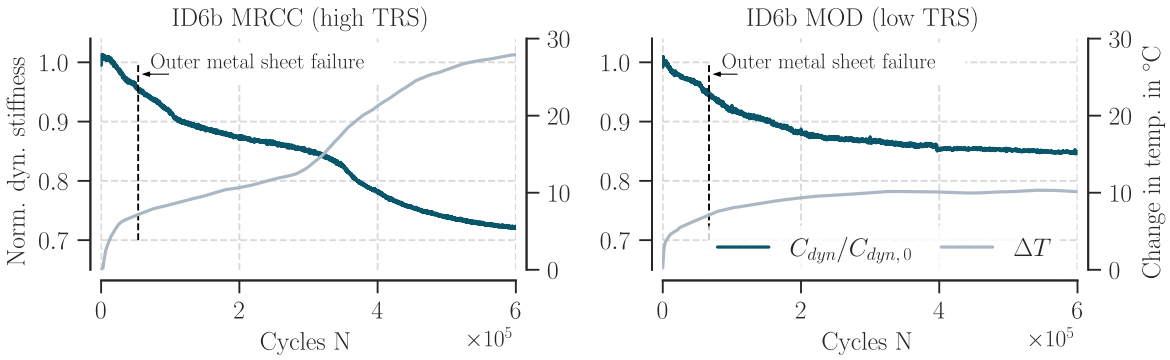

Fig. 7: Damage accumulation indicated by a decrease in normalized dynamic stiffness and an increase in specimen temperature differs for the two thermal residual stress states during cyclic testing

4. Consequences for Service-Life Prediction

Service-life predictions provide an estimation of a component's (remaining) lifespan. In the aerospace industry, structures are designed to withstand damage up to a certain size without resulting in catastrophic failure. Therefore, it is important to determine a component's residual life even after the damage has been initiated and detected by an SHM system to schedule maintenance intervals accordingly.

There are various methods available to predict the lifespan of structural components. The approaches can be clustered into three main categories, physics-based approaches (analytical/numerical), phenomenological approaches, and model-free approaches (artificial intelligence). At the same time, hybrid approaches exist, such as combining data-driven and model-based techniques in physics-informed neural networks (PINN). Physics-based methods require a detailed characterization of materials and phenomena on the micro-scale while model-free approaches need large amounts of data to be trained on. No matter which approach is chosen, all models need a certain set of input parameters to predict residual life. These input parameters may include component material and geometry, past load cycles, expected future loads, or initial defect size.

Since the component's dynamic stiffness is available from the experiments in this work, a phenomenological model developed initially by Shiri et al. [15] for composite materials is applied to the data. The model is based on the fact that damage accumulation during fatigue loading in composite materials is accompanied by a decrease in the component's stiffness as was also shown in Fig. 7. The model has proven to apply to various composite materials, layups, and stress levels in constant amplitude loading scenarios.

Since the dynamic stiffness is evaluated in this work, Shiri's model is adapted such that the cumulative damage index D(n) is correlated with the degradation of the dynamic stiffness C_{dyn} using trigonometric functions:

$$D(N) = \frac{C_{dyn,0} - C_{dyn}(N)}{C_{dyn,0} - C^*_{dyn,f}} = \frac{\sin(qx) \cdot \cos(q-p)}{\sin(q) \cdot \cos(qx-p)} \quad , \quad x = \frac{N}{N_f^*} \tag{2}$$

where $C_{dyn,0}$, $C_{dyn}(N)$, and $C^*_{dyn,f}$ are the dynamic stiffnesses during the first loading cycle N_0, the N^{th}, cycle and the final cycle before failure N_f^* and q and p are fitting parameters.

Applying the model to the measurement data requires an additional assumption. A data point at which the specimen fails is necessary since measurements are not taken until the specimen's final failure. The final data point is assumed only to change the value of the fitting parameters but not affect the model's applicability. For the sake of simplicity, a total

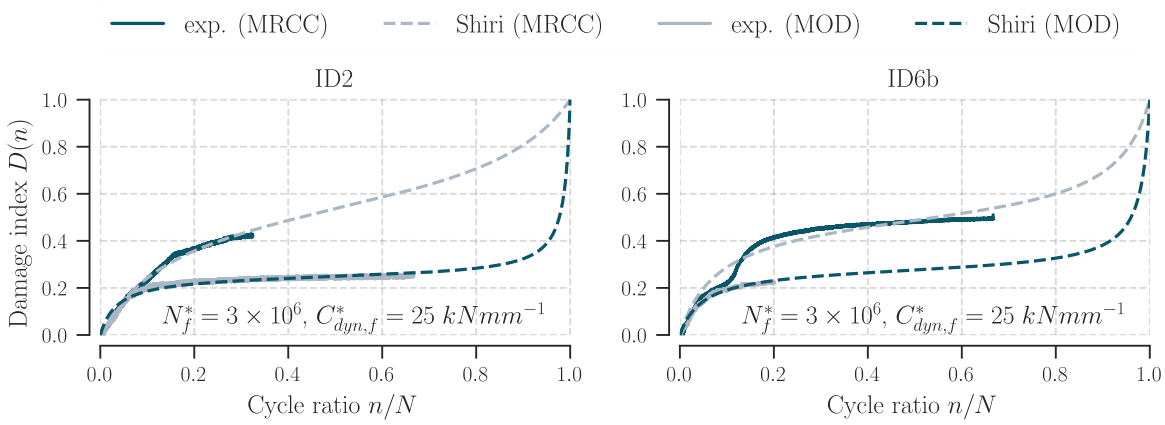

Fig. 8: Damage accumulation model of Shiri et al. [14] applied to the experimental fatigue test data

number of cycles of $N_f^* = 3 \times 10^6$ and a dynamic failure stiffness of $C_{dyn,f}^* = 25\ kN/mm$ is assumed for all specimens although an increased life for the MOD specimens is expected.

Fig. 8 shows the damage index over the cycle ratio for the two different layups and stress states. The experimental data is plotted up to the cycle count tested. The dashed lines represent the application of the model to the measured data using a non-linear least square fitting algorithm. The model can accurately describe the general trend of the damage index for all specimens and significant differences in the damage accumulation between the two TRS states can be found.

In practical applications of SHM systems, the challenge lies in obtaining the damage index. Without a tensile testing machine, the dynamic stiffness cannot be as easily determined. For composite materials, GUW-based SHM has shown that the non-linear wave propagation characteristics are a good indicator for damage accumulation inside a laminate [16]. Therefore, evaluating the non-linearity of GUW might also be a promising approach to determining the damage accumulation after a certain number of load cycles in FML. However, no matter which approach is chosen, considering the residual stress state in an FML will most likely increase the prediction accuracy, as indicated by the experimental results in this work.

Conclusions

The service life of structural components is generally determined by the external loads they are subjected to over time. However, for fiber metal laminates, an additional material effort originates from the thermal residual stress state induced during manufacturing and superimposed onto the external loads. Fatigue investigations have shown that this additional material effort significantly influences fatigue damage evolution. Under identical external loads, components with lower residual stresses experience delayed damage initiation and slower damage growth rates than specimens with higher residual stress states. These findings are independent of the layups investigated.

The results indicate that including thermally induced residual stresses in predictive approaches can enhance their accuracy in determining remaining service life. In future research, it is essential to examine which data from an SHM system can be obtained to represent the current damage accumulation in a specimen and determine the most suitable predictive model.

Funding

The authors expressly acknowledge the financial support for the research work on this article within the Research Unit 3022 “Ultrasonic Monitoring of Fibre Metal Laminates Using Integrated Sensors” and the Major Research Instrumentation Program for the high-speed thermography system (project no. 444290516) by the German Research Foundation (Deutsche Forschungsgemeinschaft (DFG)).

References

[1] Fink A. Lokale Metallhybridisierung zur Effizienzsteigerung von Hochlastfügestellen in Faserverbundwerkstoffen [Dissertation]. Braunschweig: Technische Universität Carolo-Wilhelmina zu Braunschweig; 2010.
[2] Alderliesten R. Fatigue and fracture of fibre metal laminates. Cham: Springer; 2017.
[3] Kim HS, Park SW, Lee DG. Smart cure cycle with cooling and reheating for co-cure bonded steel/carbon epoxy composite hybrid structures for reducing thermal residual stress. Composites Part A: Applied Science and Manufacturing 2006;37(10):1708–21. https://doi.org/10.1016/j.compositesa.2005.09.015.
[4] Giurgiutiu V. Structural health monitoring with piezoelectric wafer active sensors. Amsterdam: Academic Press/Elsevier; 2008.
[5] Rauter N, Mikhaylenko A, Bellam-Muralidhar NK, Lorenz D, Lammering R. Numerical simulation of guided ultrasonic waves in fiber metal laminates including model reduction methods. In: Waubke H, Balazs P, editors. Tagungsband, DAGA 2021 - 47. Jahrestagung für Akustik: 15.-18. August 2021, Wien und Online. Berlin: Deutsche Gesellschaft für Akustik e.V; 2021, p. 920–923.
[6] Maghsoodi A, Ohadi A, Sadighi M, Amindavar H. Damage detection in multilayered fiber–metal laminates using guided-wave phased array. J Mech Sci Technol 2016;30(5):2113–20. https://doi.org/10.1007/s12206-016-0418-9.
[7] Barth T, Wiedemann J, Roloff T, Hühne C, Sinapius M, Rauter N. Investigations on guided ultrasonic wave dispersion behavior in fiber metal laminates using finite element eigenvalue analysis. Proc Appl Math & Mech 2023;23(1). https://doi.org/10.1002/pamm.202200149.
[8] Rittmeier L, Rauter N, Mikhaylenko A, Lammering R, Sinapius M. The guided ultrasonic wave oscillation phase relation between the surfaces of plate-like structures of different material settings. Acoustics 2023;5(1):136–64. https://doi.org/10.3390/acoustics5010009.
[9] Wiedemann J, Barth T, Roloff T, Kluge T, Rauter N, Hühne C. Influence of residual stresses on the dispersion behavior of guided ultrasonic waves in fiber metal laminates. In: Proceedings of the 14th International Workshop on Structural Health Monitoring. Destech Publications, Inc; 2023.
[10] Barth T, Wiedemann J, Roloff T, Behrens T, Rauter N, Hühne C et al. Experimental determination of dispersion diagrams over large frequency ranges for guided ultrasonic waves in fiber metal laminates. Smart Mater. Struct. 2023;32(8):85011. https://doi.org/10.1088/1361-665X/ace0ea.
[11] Prussak R, Stefaniak D, Kappel E, Hühne C, Sinapius M. Smart cure cycles for fiber metal laminates using embedded fiber Bragg grating sensors. Composite Structures 2019;213:252–60. https://doi.org/10.1016/j.compstruct.2019.01.079.
[12] Wiedemann J, Schmidt J-UR, Hühne C. Applicability of asymmetric specimens for residual stress evaluation in fiber metal laminates. J. Compos. Sci. 2022;6(11):329. https://doi.org/10.3390/jcs6110329.
[13] Wiedemann J, Prussak R, Kappel E, Hühne C. In-situ quantification of manufacturing-induced strains in fiber metal laminates with strain gages. Composite Structures 2022;Vol. 691(1):115967. https://doi.org/10.1016/j.compstruct.2022.115967.
[14] Nettles AT. Basic mechanics of laminated composite plates: Technical report: NASA-RP-1351; Available from: https://ntrs.nasa.gov/citations/19950009349.
[15] Shiri S, Yazdani M, Pourgol-Mohammad M. A fatigue damage accumulation model based on stiffness degradation of composite materials. Materials & Design 2015;88:1290–5. https://doi.org/10.1016/j.matdes.2015.09.114.
[16] Rauter N. Analyse des Einflusses der Werkstoffdegradation auf die nichtlineare Wellenausbreitung in unidirektionalen Compositen: Experimentelle Untersuchung mit numerischer Analyse und Modellbildung: Universitätsbibliothek der HSU / UniBwH; 2017.